

Nano-Sensor for Single Cell Thermal Characterization

Salma Abdullah Binslem^a, Mohd Ridzuan Ahmad^{a,b*}

^aDept. of Control and Mechatronic Engineering, Faculty of Electrical Eng., Universiti Teknologi Malaysia, 81310 UTM Johor Bahru, Johor, Malaysia

^bInstitute of Ibnu Sina, Universiti Teknologi Malaysia, 81310 UTM Johor Bahru, Johor, Malaysia

*Corresponding author: ridzuan@fke.utm.my

Article history

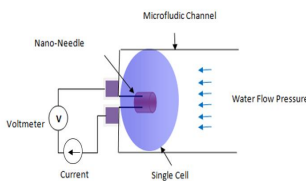
Received :5 February 2014

Received in revised form :

7 April 2014

Accepted :20 May 2014

Graphical abstract



Abstract

A cell's intracellular temperature has been shown to have a vital role in controlling the cell's properties, activities and reacting to external stimuli. Yet, current conventional methods are unable to give any measurements when spatial resolution decreases to a micro scale. Many researchers from different fields are trying to develop ways that give high accuracy and high temperature sensitivity. We present a nano-needle microfluidic system for single cell temperature measurement. Here we discuss optimization using the finite element approach to sensor design using tungsten as the electrode and semiconducting metal oxide Co_3O_4 as the sensing element. The dimensions of the sensor that gave the highest voltage and, thus, the highest sensitivity ratio of 1:4 of the electrode cross sectional area / element diameter, were a gap of 450 nm between the electrodes and a penetration depth of 250 nm of the electrode into the element. Furthermore, the voltage response had a 48 μm difference over a range of 293.15–333.15. The sensor sensitivity was a 0.01°C and the response time was 1 ns.

Keywords: Single cell; thermal properties; thermistor based nano-needle; finite element analysis

© 2014 Penerbit UTM Press. All rights reserved.

1.0 INTRODUCTION

Single cell analysis has attracted the interest of many researchers due to the significant information that can be obtained which can help improve the understanding of infections, diagnoses, response to drugs and internal pathways. Different cell properties can be studied; however, the internal temperature of a cell has shown to have important roles for the survival of cells, it also affects cell metabolism, cell division, gene expression and many other vital cellular activities¹⁻⁴. Besides, cells that are characterized with an abnormality, i.e., cancer cells, tend to have a high heat production rate⁵.

Many attempts at internal temperature measurements have been reported using different approaches, such as the use of quantum dots⁶, nano-particles⁷, and thermo sensitive materials^{8,9}. These techniques rely on the luminescent change in the sensor as a function of temperature. They tend to show a high level of sensitivity; however, several factors still discourage their use as temperature sensors in living cells, for example, the issue with photo-bleaching, the movement of material inside the cells and the possible toxicity due to material degradation¹⁰. Other attempts to measure the internal temperature of a cell can be categorized into the non-luminescent category. There are a few examples: for instance, Wang *et al.*¹¹ have designed a nano-thermocouple needle for detecting intracellular temperature with a resolution of 0.1°C ; Vyalikh *et al.*¹² have studied a multi-walled carbon nanotube as a temperature detector for biological cells. Another interesting idea is the work done by Inomata *et al.*¹³ in fabricating a microfluidic system with a resonant thermal sensor; however the application was only proven on a brown fat cell (BFC). These non-

luminescent sensors have opened the door to a new field of single-cell thermal studies that can produce sensitive temperature measurement in a very accurate and precise way.

In recent years, microfluidic devices have been developing towards improving single-cell analysis due to the various advantages they offer. They have the ability to produce a system that meets the demands of high throughput and complicated sample analysis in a reduced time¹⁴⁻¹⁶. The small dimensions of these devices encourage the consumption of small amounts of reagent, helping to control the local microenvironment, allowing the integration of multiple processing steps into a single system and reducing the cost of the traditional analysis techniques¹⁷. Here we propose a microfluidic system integrated with a nano-thermal sensor for single cell temperature measurement. However, the main focus of this paper will be on discussing the sensor's design optimization and the electro-thermal characterization of the nano-needle, highlighting the sensor's resolution and the response time.

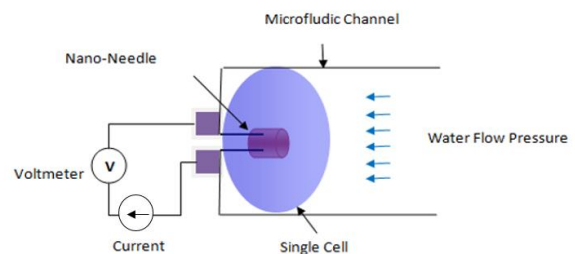


Figure 1 Schematic diagram showing the system concept

2.0 SYSTEM IDEA AND CONCEPT

The idea of the device is to integrate a thermal nano-sensor with a microfluidic channel to achieve a high throughput system with rapid analysis, targeting the internal temperature of a single biological cell. The concept can be summarized in the schematic diagram (Figure 1). By manipulating the flow of water using a syringe pump, the cells will be directed to move towards the nano-needle. The flow rate of water will be responsible for imposing the needed force on the cell to penetrate into the nano-needle for temperature measurement.

Detection is achieved by applying current to the electrodes of the nano-needle and measuring the output voltage for the results. The voltage value will change corresponding to the change in the internal temperature of the cell. The nano-needle works on the same principle as an NTC thermistor, where the semiconducting material's resistance decreases as the temperature of the surroundings (target) increases (Equation 1)

The material chosen for the electrodes was tungsten, for its high electrical conductivity and mechanical strength¹⁸, and the sensing element chosen was cobalt oxide, a transition-metal oxide, for its high temperature stability¹⁹.

$$R = R_{01}e^{\beta\left(\frac{1}{T} - \frac{1}{T_0}\right)} \quad (1)$$

where, R_{01} is the reference resistance of cobalt oxide, T refers to the temperature of the surroundings (297.15–333.15 K), T_0 is the reference temperature 298.15 K and β is the material constant of $\text{Co}_3\text{O}_4 = 7835$ ²⁰.

3.0 SIMULATION ANALYSIS

Undertaking analysis by simulation prior to fabrication or carrying out any experimental work has been a common practice in many industries, research and development units, and research in general. Simulation analysis gives several advantages, such as obtaining faster results, minimizing the cost of experiments, ensuring safety, helping to solidify the understanding of the system studied and optimizing the parameters that control the performance. However, developing a realistic model is the aspect that guarantees a successful, useful simulation, and this requires in-depth studies to obtain relevant and reliable parameters. Finite element analyses (FEAs) are numerical methods that solve partial differential equations and complex integrals which represent a system under study. In this work, ABAQUS 6.12 was used for the analysis. It is recognized for its reliability and commercialized applications.

The aim of the simulation analysis here was to obtain the sensor design that gives the highest voltage. The design was based on an NTC bead-type thermistor, thus the parameters studied were the element/electrode cross sectional area ratio, the gap between the electrodes, and the penetration depth of the electrode into the element. The other part of this study was to characterize the thermal-electric behaviour of the needle over a range of 24–60°C, to identify the sensor resolution and the response time at which it reaches equilibrium with the temperature surrounding the sensor.

3.1 Nano-needle for Design Optimization

The analysis undertaken to obtain the output voltage for dimension optimization was independent of the temperature. The total length of the sensor was set to be 3 μm , since the aim was to penetrate the centre of a yeast cell with a diameter of 6 μm . The electrical conductivity of cobalt oxide (Co_3O_4) and tungsten were

set to $18.52 \times 10^{-10} \text{ S}/\mu\text{m}^{20}$ and $18.5 \text{ S}/\mu\text{m}^{21}$, respectively. The parameters manipulated were: the ratio of electrode cross sectional area to the element diameter, the gap between the electrodes and the penetration depth of the electrodes into the element. The same current density was applied to one of the electrodes and the other was set to ground for each of the studies; the output voltages were recorded. Figure 2(A) shows a schematic diagram of the three parameters to be manipulated and Figure 2(B) shows the simulation setup to obtain the voltage output.

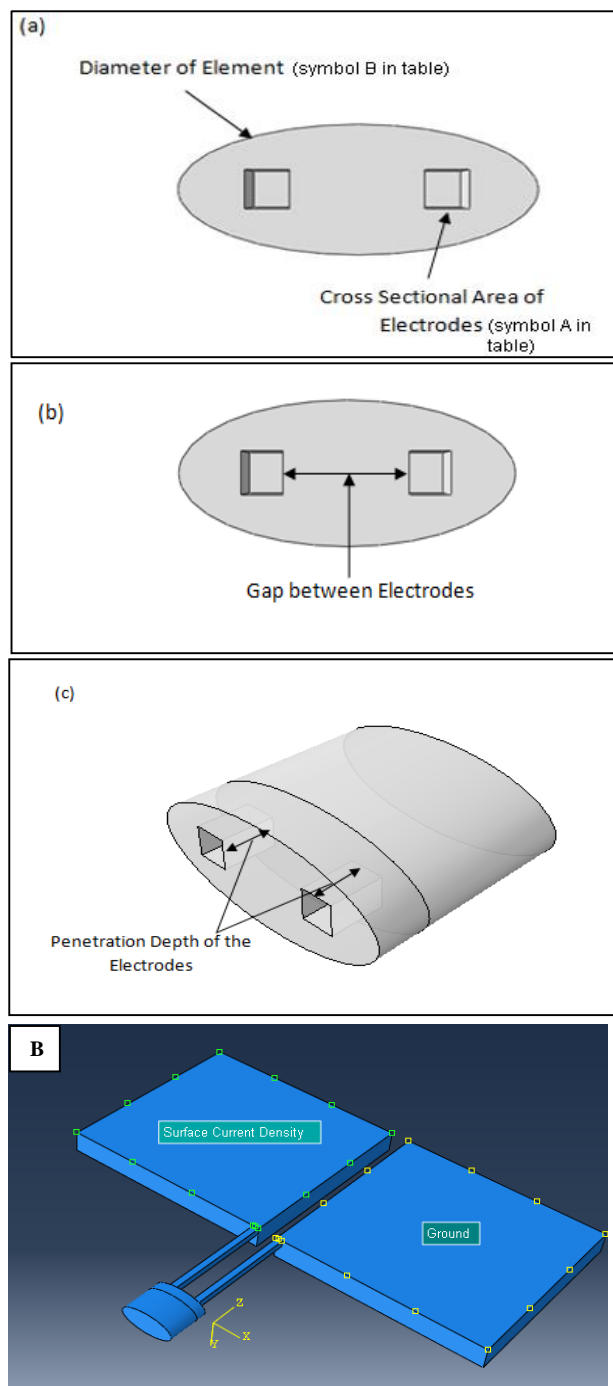


Figure 2 (A) schematic diagram of the design parameters studied. (a) Ratio of element diameter (B in Tables 2, 3 and 4) to electrode cross sectional area (A in Tables 2, 3 and 4). (b) Gap distance between electrodes. (c) Penetration depth of the electrode into the element. (B) Voltage distribution in the nano-needle

3.2 Finite Element Analysis of the Electrical Characterization of the Temperature of the Nano-needle

After optimizing the design dimensions, electrical characterizations of the sensors were carried out. Similar to the previous analysis, a model was developed based on a 3D solid deformable structure with a coupled thermal-electrical element for the analysis. The thermal analysis was used to view the voltage and its change as an effect of temperature. The density, specific heat, and thermal conductivity of cobalt oxide (Co₃O₄) and tungsten were set as given in Table 1. The resistance was calculated as a function of the temperature of Co₃O₄ using Equation (1) and for tungsten using Equation (2).

$$\rho = -1.06871 + 2.06884 \times 10^{-2} T + 1.27971 \times 10^{-6} T^2 + 8.53101 \times 10^{-9} T^3 - 5.14195 \times 10^{12} T^4 \quad (2)$$

where ρ is the resistivity of tungsten²¹.

A constant current density was applied and the voltage output was obtained as a function of temperature. The current density distribution showed a constant value over the electrodes and the sensing element. The governing equation of the whole system was Ohm's law.

4.0 RESULTS AND DISCUSSION

4.1 Results Based on the Design Optimization Analysis of the Nano-needle

Figure 3 shows the results of the simulation analysis; the colour bar indicates the voltage distribution in the model. When increasing the diameter of the element while keeping the ratio of the electrodes constant, a higher voltage value is obtained; the results are shown in Table 2. However, the increase is not very significant, thus a ratio of 1:4 was chosen to ensure minimal damage when penetrating the cell. The second study was to optimize the gap between the electrodes. The gap was varied from 250 nm to 450 nm. The results show that when increasing the gap, the voltage will proportionally increase (Table 3). Thus, a maximum gap of 450 nm was considered to have a higher voltage value. Lastly, the penetration depth of the electrode in the element was investigated; when decreasing the penetration from 750 to 250 nm, a major increase in the voltage values was observed; the results are summarized in Table 4. The final design dimensions were the following: a ratio 1:4 of the element cross sectional area to the electrode cross sectional area, a gap between the electrodes of 450 nm and a penetration depth of the electrode of 25 nm.

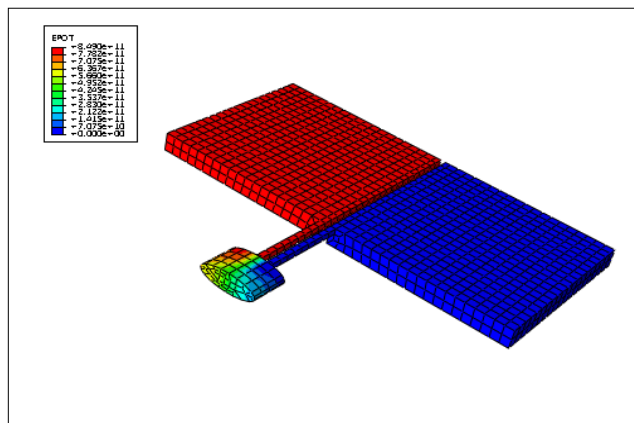


Figure 3 Voltage distribution in the nano-needle

Table 1 Input parameters for the thermal-electrical characterization

Parameter	Co3O4 ^{19,20}	Tungsten ²¹
Density (g/μm ³)	6.11e ⁻¹²	1.93e ⁻¹²
Specific heat (J/g.K)	0.513e ⁻⁹	0.1325e ⁻⁹
Thermal conductivity (W/μm.K)	25e ⁻⁶	173e ⁻⁶

Table 2 Results obtained from the element to electrode cross-sectional area

Ratio	1:4	1:5	1:6
A:B (nm)	150:600	150:750	150:900
Gap (nm)	150	150	150
Penetration depth (nm)	250	250	250
Current density (fA/μm ²)	0.1	0.1	0.1
Voltage output(μV)	15.4888	15.6364	15.9423

Table 3 Results obtained from gap manipulation studies

Ratio	1:4	1:4	1:4
A:B (nm)	150:600	150:600	150:600
Gap (nm)	150	300	450
Penetration depth (nm)	500	500	500
Current density (fA/μm ²)	0.1	0.1	0.1
Voltage output(μV)	15.4888	25.3583	34.2343

Table 4 Results obtained from penetration depth manipulation studies

Ratio	1:4	1:4	1:4
A:B (nm)	150:600	150:600	150:600
Gap (nm)	450	450	450
Penetration depth (nm)	250	500	750
Current density (fA/μm ²)	0.1	0.1	0.1
Voltage output(μV)	25.1103e+2	34.2343	26.969

4.2 Results Based on the Electrical-thermal Characterization of the Nano-Needle

Thermal-electric characterization has been undertaken in order to characterize the needle performance. A plot of the voltage change as a function of temperature, ranging from 293.15–333.15 K, is shown in Figure 4. The behaviour of the graph as predicted shows typical NTC thermistor behaviour; a decrease in voltage as the temperature increases. The results showed that the sensor is able to detect the temperature in the required range having a significant difference of approximately 48 μV between the highest and the lowest voltage. Furthermore, in order to determine the sensitivity of the sensor, a change of 0.01°C has been tested to obtain the voltage change. Figure 5 shows a plot of the voltage vs. temperature ranging from 307.15–307.25 K. Although the voltage decrease with the temperature does not present a linear graph, the R^2 value of the trend line is 0.97 which is an acceptable percentage error. Thus the sensor is able to detect a very small change in temperature reaching up to 0.01°C; this makes it a good candidate for real-time monitoring applications. Another study was to examine how fast the sensor responds and reaches equilibrium with the surrounding temperature. The surrounding temperature was set to 293.16 K and the initial temperature of the sensor was set to be 293.15 K, corresponding to a 0.01°C increase. From the results in Figure 6, that sensor response was shown to be very fast and reached equilibrium with the surroundings in 1 ns. The results presented show that the sensor can react to temperature very quickly with high sensitivity, which is very important in single-cell temperature measurements.

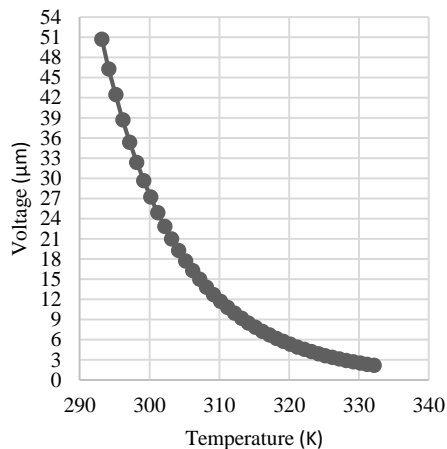


Figure 4 Voltage change with the temperature range 293.15-333.15K

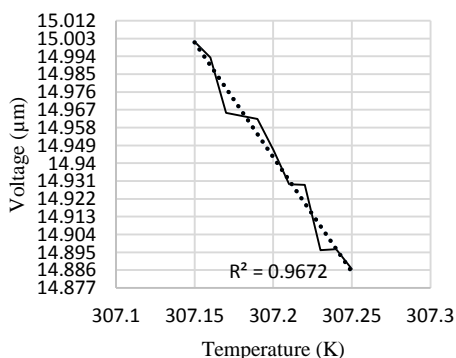


Figure 5 Voltage change with temperature range 307.15–307.25 K

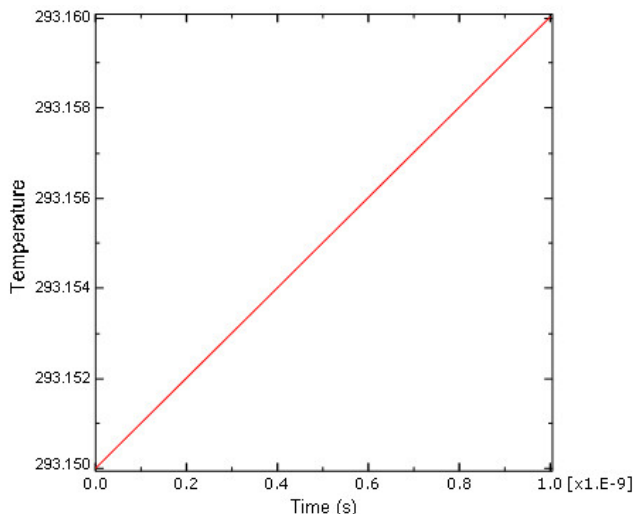


Figure 6 Temperature response to the surrounding temperature

5.0 CONCLUSION

Intracellular temperature production in cells is strongly affected by diseases. For instance, cells which are diagnosed with cancer have a higher temperature because of their rapid metabolism. Knowing cell temperature has advantages for cell signalling studies, cell metabolism, disease diagnosis, and therapeutic effect evaluations. This paper discusses the development of a nano-needle thermal sensor for single-cell temperature measurement. A design optimization study has been undertaken as well as electrical-thermal characterization of the sensor. Furthermore, all the required parameters for the modelling have been included for accurate analysis. The final design dimensions have been chosen to have the highest voltage yet causing minimum damage to the cell after penetration. Moreover, the electrical-thermal characterization showed that the nano-needle has the ability to obtain the output voltage for temperature changes of 0.01 °C in the range of 24–60°C, which is considered to be reliably accurate and can give a real-time reading of cell temperature if exposed to any disturbance. The sensor response to surrounding temperature was 1 ns. Further studies will be undertaken to achieve a high throughput system with high accuracy to obtain real-time cell temperature measurement.

Acknowledgements

We would like to express our appreciation to the Ministry of Higher Education Malaysia (MOHE) grant no 78677 (FRGS), (MOHE) grant No. 4L038 (ERGS) and Universiti Teknologi Malaysia, grant Nos. 77973 (NAS), 03H80 (GUP) and 02H34 (GUP) for funding this project and for their endless support.

References

- [1] D. Evanko. 2012. Sensors and Probes: A Thermometer for Cells. *Nature Methods*. 9(4): 328–328.
- [2] K. M. McCabe and M. Hernandez. 2011. Molecular Thermometry. *NIH Public Access*. 67(5): 469–475.
- [3] S. Li, K. Zhang, J.-M. Yang, L. Lin, and H. Yang. 2007. Single Quantum Dots as Local Temperature Markers. *Nano Letters*. 7(10): 3102–5.
- [4] D. Evanko. 2012. Sensors and Probes: A Thermometer for Cells. *Nature Methods*. 9(4): 328–328.
- [5] J. S. Donner, S.A.a Thompson, M. P. Kreuzer, G. Baffou, and R. Quidant. 2012. Mapping Intracellular Temperature Using Green Fluorescent Protein. *Nano Letters*. 12(4): 2107–11.

- [6] J.-M. Y. J.-M. Yang, H. Y. H. Yang, and L. L. L. Lin. 2010. Thermogenesis Detection of Single Living Cells via Quantum Dots. In *Micro Electro Mechanical Systems MEMS 2010 IEEE 23rd International Conference on*. 963–966
- [7] J. Lee, A. O. Govorov, and N. A. Kotov. 2005. Nanoparticle Assemblies with Molecular Springs: A Nanoscale Thermometer. *Angewandte Chemie*. 117(45): 7605–7608.
- [8] C. Espenel, M.-C. Giocondi, B. Seantier, P. Dosset, P.-E. Milhiet, and C. Le Grimellec. 2008. Temperature-dependent Imaging of Living Cells by AFM. *Ultramicroscopy*. 108(10): 1174–80.
- [9] C. Gota, K. Okabe, T. Funatsu, Y. Harada, and S. Uchiyama. 2009. Hydrophilic Fluorescent Nanogel Thermometer for Intracellular Thermometry. *Journal of the American Chemical Society*. 131(8): 2766–7.
- [10] C. D. S. Brites, P. P. Lima, N. J. O. Silva, A. Millán, V. S. Amaral, F. Palacio, and L. D. Carlos. 2012. Thermometry at the Nanoscale. *Nanoscale*. 4(16): 4799–829.
- [11] C. Wang, R. Xu, W. Tian, X. Jiang, Z. Cui, M. Wang, H. Sun, K. Fang, and N. Gu. 2011. Determining Intracellular Temperature at Single-cell Level by a Novel Thermocouple Method. *Cell Research*. 21(10): 1517–9.
- [12] A. Vyalikh, A. U. B. Wolter, S. Hampel, D. Haase, M. Ritschel, A. Leonhardt, H.-J. Grafe, A. Taylor, K. Krämer, B. Büchner, and R. Klingeler. 2008. A Carbon-wrapped Nanoscaled Thermometer for Temperature Control in Biological Environments. *Nanomedicine*. 3(3): 321–7.
- [13] N. Inomata, M. Toda, M. Sato, A. Ishijima, and T. Ono. 2012. Pico Calorimeter for Detection of Heat Produced in an Individual Brown Fat Cell. *Applied Physics Letters*. 100(15): 154104.
- [14] D. Gao, H. Liu, Y. Jiang, and J.-M. Lin. 2013. Recent Advances in Microfluidics Combined with Mass Spectrometry: Technologies and Applications. *Lab on a Chip*. 13(17): 3309–22.
- [15] Y. Zheng, J. Nguyen, Y. Wei, and Y. Sun. 2013. Recent Advances in Microfluidic Techniques for Single-cell Biophysical Characterization. *Lab on a chip*. 13(13): 2464–83.
- [16] M. Fortier, E. Bonneil, P. Goodley, P. Thibault, and C. Pharmaceuticals. 2005. Integrated Microfluidic Device for Mass Spectrometry-based Proteomics and Its Application to Biomarker Discovery Programs. *Analytical Chemistry*. 77(6): 1631–1640.
- [17] V. Lecault, A. K. White, A. Singhal, and C. L. Hansen. 2012. Microfluidic Single Cell Analysis: From Promise to Practice. *Current Opinion in Chemical Biology*. 16(3–4): 381–90.
- [18] Ahmad, M. R. Nakajima, M., Kojima, M., Kojima, S., Homma, M., & Fukuda, T. 2012. Instantaneous and Quantitative Single Cells Viability Determination Using Dual Nanoprobe Inside ESEM. *Nanotechnology, IEEE Transactions on*. 11(2): 298–306.
- [19] Sahoo, P., Djieutedjeu, H. & Poudeu, P. F. P. 2013. Co3O4 nanostructures: The Effect of Synthesis Conditions on Particles Size, Magnetism and Transport Properties. *J. Mater. Chem. A1*: 15022.
- [20] Liang, S., Gao, J. Q., Yang, J. F. & Luo, M. 2008. The Resistivity-Temperature Property of Transition Metal Oxide Co3O4 with In2O3. Addition. *Mater. Sci. Forum*. 569: 193–196.
- [21] Tritt, T. M. 2004. *Thermal Conductivity: Theory, Properties, and Applications*. (Springer) <http://books.google.com.my/books?id=I9XRU9mtBeoC>.